

Ultrafast Phenomena V

Proceedings of the Fifth OSA Topical Meeting
Snowmass, Colorado, June 16–19, 1986

Editors: G.R. Fleming and A.E. Siegman

With 427 Figures

Springer-Verlag Berlin Heidelberg New York
London Paris Tokyo

Contents

| | | |
|---|---|----|
| Part I | Mode Locking and Ultrashort Pulse Generation | |
| <hr/> | | |
| Passive and Hybrid Femtosecond Operation of a Linear Astigmatism Compensated Dye Laser By J.-C. Diels, N. Jamasbi, and L. Sarger (With 1 Figure) | | 2 |
| Generation of 55-fs Pulses and Variable Spectral Windowing in a Linear-Cavity Synchronously Pumped cw Dye Laser By M.D. Dawson, T.F. Boggess, D.W. Garvey, and A.L. Smirl (With 4 Figures) | | 5 |
| Cavity-Mirror Dispersion Dependence of Pulse Duration Generated from a Simple CPM Laser: An Experimental Study By M. Yamashita, K. Torizuka, T. Sato, and M. Ishikawa (With 2 Figures) | | 8 |
| Femtosecond Pulse Generation from Passively Mode Locked Continuous Wave Dye Lasers 550–700 nm By P.M.W. French and J.R. Taylor (With 3 Figures) | | 11 |
| Stabilisation of a CPM Dye Laser Synchronously Pumped by a Frequency Doubled ML YAG Laser By J. Chesnoy and L. Fini (With 3 Figures) | | 14 |
| Fluctuations and Chirp in Colliding-Pulse Mode-Locked Dye Lasers. By D. Kühlke, T. Bonkhofer, U. Herpers, and D. von der Linde (With 2 Figures) | | 17 |
| Experimental Observation of High Order Solitons in a Colliding Pulse Mode-Locked Laser By F. Salin, P. Grangier, G. Roger, and A. Brun (With 4 Figures) | | 20 |
| Advances in the Theory of Mode-Locking by Synchronous Pumping. By G.H.C. New and J.M. Catherall (With 3 Figures) ... | | 24 |
| Collective Modes - An Analytical Model for Active Mode Locking in the Transient Case By P. Aechtner, P. Heinz, and A. Laubereau (With 2 Figures) | | 27 |

| | |
|--|----|
| Generation of Picosecond Pulses from a Continuous Wave Neodymium:Phosphate Glass Laser By L. Yan, J.D. Ling, P.-T. Ho, and C.H. Lee (With 3 Figures) | 30 |
|--|----|

Part II Ultrafast Optical Generation and Measurement Techniques

| | |
|---|----|
| Fourier Transform Picosecond Pulse Shaping and Spectral Phase Measurement in a Grating Pulse-Compressor. By J.P. Heritage, A.M. Weiner, and R.N. Thurston (With 4 Figures) | 34 |
| Picosecond Pulse Amplification Using Pulse Compression Techniques. By D. Strickland, P. Maine, M. Bouvier, S. Williamson, and G. Mourou (With 4 Figures) | 38 |
| New Optical Design for a Jet Amplifier. By O. Seddiki, A. Goddi, R. Mounet, J.-F. Morhange, and C. Hirlimann (With 2 Figures) ... | 43 |
| Fiber Raman Amplification Soliton Laser (FRASL) By M.N. Islam, L.F. Mollenauer, and R.H. Stolen (With 4 Figures) | 46 |
| Dispersion Compensated Fiber Raman Oscillator By J.D. Kafka, D.F. Head, and T. Baer (With 2 Figures) | 51 |
| 80-fs Soliton-like Pulses from an Optical Nonlinear Fiber Resonator. By B. Zysset, P. Beaud, W. Hodel, and H.P. Weber (With 4 Figures) | 54 |
| The Stabilized Soliton Laser By F.M. Mitschke and L.F. Mollenauer (With 4 Figures) | 58 |
| The Soliton Self Frequency Shift. By F.M. Mitschke, L.F. Mollenauer, and J.P. Gordon (With 2 Figures) | 62 |
| Solitons at the Zero Dispersion Wavelength of Single-Mode Fibers By P.K.A. Wai, C.R. Menyuk, H.H. Chen, and Y.C. Lee (With 1 Figure) | 65 |
| Active Mode-Locking of an InGaAsP Optical-Fiber Ring Laser By G. Eisenstein, R.M. Jopson, M.S. Whalen, K.L. Hall, and G. Raybon (With 4 Figures) | 68 |
| Femtosecond Resolved Fluorescence By W. Rudolph and J.-C. Diels (With 2 Figures) | 71 |
| Parametric Amplification Sampling Spectroscopy (PASS): A New Technique for Resolving Near-Infrared Luminescence on a Subpicosecond Time Scale. By D. Hulin, A. Migus, A. Antonetti, I. Ledoux, J. Badan, and J. Zyss (With 3 Figures) | 75 |

| | |
|--|----|
| Measurement of Optical Phase with Subpicosecond Resolution by Time Domain Interferometry. By J.E. Rothenberg (With 6 Figures) | 78 |
| Real Time Picosecond Optical Oscilloscope By J.A. Valdmanis (With 8 Figures) | 82 |
| Beam Overlap for Long Delay Lines Using Active Feedback By C. Doland, W.B. Jackson, and A. Andersson (With 3 Figures) . | 86 |
| Ultrashort Dye Laser Pulses Using the Sweeping Oscillator Method. By Y.H. Meyer, M.M. Martin, E. Br  h  ret, and O. Benoit d'Azy (With 4 Figures) | 89 |
| An Investigation on Ultrashort Light Pulse Generation by Travelling-Wave Amplified Spontaneous Emission By W. Lee, C. Ning, Z. Huang, and W. Wang (With 5 Figures) ... | 92 |

Part III Electrooptic Sampling Techniques

| | |
|--|-----|
| Electrooptic Sampling of Gallium Arsenide Integrated Circuits By K.J. Weingarten, M.J.W. Rodwell, J.L. Freeman, S.K. Diamond, and D.M. Bloom (With 6 Figures) | 98 |
| Picosecond Characterization of Ultrafast Phenomena: New Devices and New Techniques. By D.R. Dykaar, R. Sobolewski, J.F. Whitaker, T.Y. Hsiang, G.A. Mourou, M.A. Hollis, B.J. Clifton, K.B. Nichols, C.O. Bozler, and R.A. Murphy (With 4 Figures) | 103 |
| Precise Measurement of Signal Propagation Characteristics in GaAs Integrated Circuits by Picosecond Electro-Optic Sampling By R.K. Jain, X.-C. Zhang, M.G. Ressler, and T.J. Pier (With 2 Figures) | 107 |
| Propagation of Ultrashort Electrical Pulses on Superconducting Transmission Lines By I.N. Duling III, C.-C. Chi, W.J. Gallagher, D. Grischkowsky, N.J. Halas, M.B. Ketchen, and A.W. Kleinsasser (With 4 Figures) | 110 |
| High Repetition Rate Electro-Optic Sampling with an Injection Laser. By A.J. Taylor, R.S. Tucker, J.M. Wiesenfeld, G. Eisenstein, and C.A. Burrus (With 5 Figures) | 114 |
| Picosecond Optoelectronic Sampling of Electrical Waveforms Produced by an Optically Excited Field Effect Transistor By D.E. Cooper and S.C. Moss (With 1 Figure) | 117 |

| | |
|--|-----|
| Picosecond Electrical Pulses in Microelectronics. By P.G. May, G.P. Li, J.-M. Halbout, M.B. Ketchen, C.-C. Chi, M. Scheuermann, I.N. Duling III, D. Grischkowsky, and M. Smyth (With 3 Figures) . | 120 |
| High Speed Circuit Measurements Using Photoemission Sampling By J. Bokor, A.M. Johnson, R.H. Storz, and W.M. Simpson (With 2 Figures) | 123 |
| Photoemissive Sampling of Picosecond Electrical Waveforms By A.M. Weiner, R.B. Marcus, P.S.D. Lin, and J.H. Abeles (With 5 Figures) | 127 |
| Nonlinear Responses of Picosecond Photodetectors to Photogenerated Carriers By T.F. Carruthers and J.F. Weller (With 3 Figures) | 131 |
| Direct Generation of Picosecond to Subpicosecond Optical Pulses Using Electrooptic Modulation Methods By T. Kobayashi, A. Morimoto, T. Fujita, K. Amano, T. Uemura, and T. Sueta (With 6 Figures) | 134 |
| Elimination of Dynamic Flash in a Picosecond Streak Image Tube By Huanwen Zhang (With 1 Figure) | 137 |

Part IV **Nonlinear Optics and Continuum Generation**

| | |
|---|-----|
| Parametric Chirp Reversal and Enhancement: Application in Femtosecond Optics. By A. Piskarskas, D. Podenas, A. Stabinis, A. Umbrasas, A. Varanavichius, A. Yankauskas, and G. Yonushauskas (With 7 Figures) | 142 |
| Supercontinuum Generation in Gases: A High Order Nonlinear Optics Phenomenon. By P.B. Corkum, C. Rolland, and T. Srinivasan-Rao (With 3 Figures) | 149 |
| New Excitation and Probe Continuum Sources for Subpicosecond Absorption Spectroscopy By J.H. Glownia, J. Misewich, and P.P. Sorokin (With 2 Figures) . | 153 |
| Induced Phase Modulation and Spectral Broadening of a Weak 530-nm Picosecond Pulse by an Intense 1060-nm Picosecond Pulse in Glass. By R.R. Alfano, Q.X. Li, T. Jimbo, J.T. Manassah, and P.P. Ho (With 2 Figures) | 157 |
| The Observation of Chirped Stimulated Raman Scattered Light in Fibers. By A.M. Johnson, R.H. Stolen, and W.M. Simpson (With 3 Figures) | 160 |

| | |
|---|-----|
| Observation of 7.2-THz Beats Between the D-Lines of Atomic Rb By J.E. Golub and T.W. Mossberg (With 1 Figure) | 164 |
| Coherent Multiphoton Resonant Interaction and Harmonic Generation. By A. Mukherjee, N. Mukherjee, J.-C. Diels, and G. Arzumanyan (With 4 Figures) | 166 |
| Ultrafast Chaos from Semiconductor Lasers. By Y. Cho, T. Umeda, I. Jun Cha, M. Koishi, and M. Miwa (With 5 Figures) . | 169 |

**Part V Applications to Semiconductors, Quantum Wells, and
 Solid State Physics**

| | |
|--|-----|
| Thermodynamics and Kinetics of Melting, Evaporation and Crystallization, Induced by Picosecond Pulsed Laser Irradiation By F. Spaepen (With 1 Figure) | 174 |
| Investigation of Nonthermal Population Distributions with 10-fs Optical Pulses. By C.V. Shank, R.L. Fork, C.H. Brito Cruz, and W. Knox (With 3 Figures) | 179 |
| Superheating During Ultrafast Laser Heating of Semiconductors By D. von der Linde, N. Fabricius, B. Danielzik, and P. Hermes (With 4 Figures) | 182 |
| Non-equilibrium Carriers in GaAs: Secondary Emission During the First Two Picoseconds By J.A. Kash and J.C. Tsang (With 5 Figures) | 188 |
| Ultrafast Carrier Dynamics in GaAs and $Al_xGa_{1-x}As$ By W.Z. Lin, J.G. Fujimoto, E.P. Ippen, and R.A. Logan (With 4 Figures) | 193 |
| Subpicosecond Optical Non-linearities in GaAs Multiple-Quantum- Well Structures. By D. Hulin, A. Antonetti, A. Migus, A. Mysyrowicz, H.M. Gibbs, N. Peyghambarian, W.T. Masselink, and H. Morkoç (With 5 Figures) | 197 |
| Picosecond Relaxation of Nonthermal Wannier Excitons in GaAs By L. Schultheis, J. Kuhl, A. Honold, and C.W. Tu (With 1 Figure) | 201 |
| Picosecond Observation of the Photorefractive Effect in GaAs By A.L. Smirl, G.C. Valley, M.B. Klein, K. Bohnert, and T.F. Boggess (With 2 Figures) | 203 |

| | |
|--|-----|
| Time-Resolved Photoluminescence Measurements in $\text{Al}_x\text{Ga}_{1-x}\text{As}$ Under Intense Picosecond Excitation By K. Bohnert, H. Kalt, D.P. Norwood, T.F. Boggess, A.L. Smirl, and R.Y. Loo (With 2 Figures) | 207 |
| Picosecond Excite-Probe and Transient Grating Studies of $\text{Ga}_x\text{In}_{1-x}\text{As}_y\text{P}_{1-y}$. By R.J. Manning, A. Miller, A.M. Fox, and J.H. Marsh (With 2 Figures) | 210 |
| Ultrafast Dynamics in GaAlAs Diode Laser Amplifiers By M.S. Stix, M.P. Kesler, and E.P. Ippen (With 8 Figures) | 213 |
| Electronic Energy Relaxation and Localization in Two II-VI Compound Semiconductor Quantum Well Structures By Y. Hefetz, W.C. Goltsov, D. Lee, and A.V. Nurmikko (With 6 Figures) | 218 |
| Transient Raman Scattering in Multiple Quantum Well Structures By D.Y. Oberli, D.R. Wake, M.V. Klein, J. Klem, and H. Morkoç (With 2 Figures) | 223 |
| Fast Energy Relaxation of Hot Electrons in Bulk GaAs and Multi- Quantum Wells. By C.H. Yang and S.A. Lyon (With 2 Figures) ... | 227 |
| Picosecond Photoluminescence and Energy-Loss Rates in GaAs Quantum Wells Under High-Density Excitation By T. Kobayashi, H. Uchiki, Y. Arakawa, and H. Sakaki (With 4 Figures) | 231 |
| Broad Tuning of the Photoluminescence Energy and Lifetime by the Quantum-Confined Stark Effect. By H.-J. Polland, L. Schultheis, J. Kuhl, E.O. Göbel, and C.W. Tu (With 2 Figures) | 234 |
| Auger Heating of Silicon-on-Sapphire by Femtosecond Optical Pulses. By M.C. Downer and C.V. Shank (With 2 Figures) | 238 |
| The Origin of Picosecond Photoinduced Absorption Decays in Hydrogenated Amorphous Silicon By W.B. Jackson, C. Doland, and C.C. Tsai (With 2 Figures) | 242 |
| Picosecond Decay of Photoinduced Absorption in Hydrogenated Amorphous Silicon By D.M. Roberts and T.L. Gustafson (With 2 Figures) | 245 |
| Femtosecond Spectroscopy of Hot Carriers in Germanium By P.M. Fauchet, D. Hulin, G. Hamoniaux, A. Orszag, J. Kolodzey, and S. Wagner (With 3 Figures) | 248 |

| | |
|---|-----|
| Spin Dephasing Kinetics of Free Carriers in Alloy Semimagnetic Semiconductors $Cd_{1-x}Mn_xSe$ by One and Two Photon Excitation By M.R. Junnarkar and R.R. Alfano (With 1 Figure) | 251 |
| Detection of Higher Order Fourier Components of Index Gratings in Picosecond Transient Grating Experiments By E.O. Göbel and H. Saito (With 3 Figures) | 254 |
| Transient Thermoreflectance Studies of Thermal Transport in Compositionally Modulated Metal Films. By G.L. Eesley, C.A. Paddock, and B.M. Clemens (With 2 Figures) | 257 |
| Femtosecond Studies of Nonequilibrium Electronic Processes in Metals. By R.W. Schoenlein, W.Z. Lin, J.G. Fujimoto, and G.L. Eesley (With 4 Figures) | 260 |
| Time-Resolved Observation of Electron-Phonon Relaxation During Femtosecond Laser Heating of Copper. By H. Elsayed-Ali, M. Pessot, T. Norris, and G. Mourou (With 2 Figures) | 264 |
| Femtosecond Carrier Relaxation in Semiconductor-Doped Glasses By M.C. Nuss, W. Zinth, and W. Kaiser (With 2 Figures) | 267 |
| Femtosecond Dynamics of Electron-Hole Plasma in Semiconductor Microcrystallite Doped Glass. By G.R. Olbright, B.D. Fluegel, S.W. Koch, and N. Peyghambarian (With 2 Figures) | 270 |
| High-Contrast Ultrafast Phase Conjugation in Semiconductor-Doped Glass. By D. Cotter (With 3 Figures) | 274 |
| Femtosecond Vibrational Relaxation of the $F\frac{1}{2}$ Center in LiF By W.H. Knox, L.F. Mollenauer, and R.L. Fork (With 2 Figures) . | 277 |
| Determination of the Rapid Quenching Rates of Excited State F-Centers by OH^- Defects in KCl. By Du-Jeon Jang, T.C. Corcoran, M.A. El-Sayed, L. Gomes, and F. Luty (With 4 Figures) | 280 |
| Propagation of Coherent Phonon Polaritons in $LiTaO_3$ Measured by FIR-Cherenkov-Pulses By M.C. Nuss and D.H. Auston (With 3 Figures) | 284 |

Part VI Chemical Reaction Dynamics

| | |
|---|-----|
| Cages, Crossings and Correlations – Theoretical Perspectives on Solution Reaction Dynamics. By J.T. Hynes | 288 |
|---|-----|

| | |
|---|-----|
| Polarity Dependent Barriers and the Photoisomerization Dynamics of Polar Molecules in Solution. By J.M. Hicks, M.T. Vandersall, E.V. Sitzmann, and K.B. Eisenthal (With 3 Figures) | 293 |
| Dynamic Solvent Effects on Small Barrier Isomerizations By P.F. Barbara and V. Nagarajan (With 3 Figures) | 299 |
| Solvation Dynamics in Polar Liquids: Experiment and Simulation By M. Maroncelli, E.W. Castner, Jr., S.P. Webb, and G.R. Fleming (With 4 Figures) | 303 |
| Femtosecond Study of Electron Localization and Solvation in Pure Water. By Y. Gauduel, J.L. Martin, A. Migus, N. Yamada, and A. Antonetti (With 2 Figures) | 308 |
| Time-Dependent Fluorescence Shift in Alcoholic Solvents: A Non-Debye Behaviour Related to Hydrogen Bonds By C. Rullière, A. Declémy, and Ph. Kottis (With 4 Figures) | 312 |
| Picosecond Dynamics of Proton-Anion Ion Pair Geminate Recombination. By D. Huppert and E. Pines (With 1 Figure) | 315 |
| Excited State Proton Transfer in Matrix Isolated Water and Methanol Complexes of 2-Hydroxy-4,5-benzotropone and 3-Hydroxyflavone By D.F. Kelley and G.A. Brucker (With 2 Figures) | 319 |
| Detection of the Inverted Region in Photo-induced Intramolecular Electron Transfer. By R.J. Harrison, G.S. Beddard, J.A. Cowan, and J.K.M. Sanders (With 2 Figures) | 322 |
| Ultrafast Studies Designed to Test the Fundamental Statistical Assumptions Underlying Chemical Reactivity in Liquids By C.B. Harris, J.K. Brown, M.E. Paige, D.E. Smith, and D.J. Russell (With 4 Figures) | 326 |
| Geminate Recombination and Relaxation of Condensed Phase Molecular Halogens By D.F. Kelley and N.A. Abul Haj (With 1 Figure) | 330 |
| Fast Photochemical Processes of Aromatic Nitro Compounds in Solution. By B.B. Craig, S.K. Chattopadhyay, and J.C. Mialocq (With 4 Figures) | 334 |
| Cage Recombination and Unimolecular β -Scission Reactions of Sulfur Centered Free Radicals By T.W. Scott and S.N. Liu (With 3 Figures) | 338 |

| | |
|--|-----|
| The Influence of Friction and Deuteration on Stilbene Isomerization. By S.H. Courtney, M.W. Balk, S. Canonica, S.K. Kim, and G.R. Fleming (With 3 Figures) | 341 |
| Kramers-Hubbard Approach to the Solvent Dependence of Isomerization. By M. Lee and R.M. Hochstrasser (With 3 Figures) | 344 |
| Photoisomerization Studies of Substituted Stilbenes: 4,4'-Dihydroxystilbene and 4,4'-Dimethoxystilbene By D.M. Zeglinski and D.H. Waldeck (With 2 Figures) | 347 |
| Picosecond Studies of Barrierless Torsional Diffusion By D. Ben-Amotz and C.B. Harris (With 2 Figures) | 350 |
| Time-Resolved Fluorescence Spectra of Ethidium Bromide By J.H. Sommer, T.M. Nordlund, M. McGuire, and G. McLendon (With 3 Figures) | 353 |
| Picosecond and Femtosecond Molecular Beam Chemistry: Coherence and Fragment Recoil Dynamics By A.H. Zewail (With 4 Figures) | 356 |
| Picosecond Laser Study of the Collisionless UV Photodissociation of Energetic Materials By J.-C. Mialocq and J.C. Stephenson (With 3 Figures) | 362 |
| Experimental Study of Harmonic Generation with Picosecond 248 nm Radiation. By T.S. Luk, A. McPherson, H. Jara, U. Johann, I.A. McIntyre, A.P. Schwarzenbach, K. Boyer, and C.K. Rhodes (With 2 Figures) | 366 |
| Time-Resolved Measurement of Laser-Induced Desorption of a Molecular Monolayer. By G. Arjavalingam, T.F. Heinz, and J.H. Glowonia (With 1 Figure) | 370 |

Part VII Dynamics of Biological Processes

| | |
|---|-----|
| Picosecond Electron Transfer and Stimulated Emission in Reaction Centers of <i>Rhodobacter sphaeroides</i> and <i>Chlorofelxus aurantiacus</i> . By M. Becker, D. Middendorf, N.W. Woodbury, W.W. Parson, and R.E. Blankenship (With 4 Figures) | 374 |
| Femtosecond Spectroscopy of the Primary Events of Bacterial Photosynthesis By W. Zinth, J. Dobler, and W. Kaiser (With 3 Figures) | 379 |
| An Accumulated Photon Echo Study of Sub-picosecond Processes in Photosynthetic Reaction Centers By S.R. Meech, A.J. Hoff, and D.A. Wiersma (With 2 Figures) | 384 |

| | |
|---|-----|
| Ultrafast Electron and Energy Transfer in Reaction Center and Antenna Proteins from Photosynthetic Bacteria By M.R. Wasielewski, D.M. Tiede, and H.A. Frank (With 5 Figures) | 388 |
| Femtosecond Spectroscopy of Excitation Energy Transfer and Initial Charge Separation in the Reaction Center of the Photosynthetic Bacterium <i>Rhodospseudomonas sphaeroides</i> By J. Breton, J.-L. Martin, A. Migus, A. Antonetti, and A. Orszag (With 4 Figures) | 393 |
| Picosecond Transient Absorption Spectroscopy of Green Plant Photosystem I Reaction Centres By B.L. Gore, L.B. Giorgi, and G. Porter (With 1 Figure) | 398 |
| Femtosecond-Pulse Spectroscopy of Primary Photoprocesses in Reaction Centers of <i>Rhodospseudomonas sphaeroides</i> R-26 By S.V. Chekalin, Yu.A. Matveets, and A.P. Yartsev (With 3 Figures) | 402 |
| Detergent Effects upon the Picosecond Dynamics of Higher Plant Light Harvesting Chlorophyll Complex (LHC). By J.P. Ide, D.R. Klug, W. Kuhlbrandt, G. Porter, and J. Barber (With 1 Figure) | 406 |
| Picosecond Conformational Intermediates in the Bacteriorhodopsin Photocycle. By G.H. Atkinson, T.L. Brack, D. Blanchard, G. Rumbles, and L. Siemankowski (With 3 Figures) | 409 |
| Electron Transfer and Rapid Restricted Motion in Homologous Azurins. By J.W. Petrich, J.W. Longworth, and G.R. Fleming (With 3 Figures) | 413 |
| Primary Process of Vision: Hypsorhodopsin By T. Kobayashi, H. Ohtani, and M. Tsuda (With 3 Figures) | 416 |
| Reactivity and Dynamics of Hemeproteins in the Femtosecond and Picosecond Time Domains. By D. Houde, J.W. Petrich, O.L. Rojas, C. Poyart, A. Antonetti, and J.L. Martin (With 3 Figures) | 419 |
| Picosecond Raman Hole Burning as a Probe of Conformational Heterogeneity: Applications to Oxyhemoglobin By B.F. Campbell and J.M. Friedman (With 4 Figures) | 423 |
| Ultrafast Studies of Nitrosylmyoglobin. By K.A. Jongeward, J.C. Marsters, and D. Magde (With 4 Figures) | 427 |
| Molecular Dynamics Study of Vibrational Cooling in Optically Excited Hemeproteins. By E.R. Henry, W.A. Eaton, and R.M. Hochstrasser (With 1 Figure) | 430 |

| | |
|--|-----|
| Chemical Reaction in a Glassy Matrix: Dynamics of Ligand Binding to Protoheme in Glycerol:Water. By J.R. Hill, M.J. Cote, D.D. Dlott, J.F. Kauffman, J.D. McDonald, P.J. Steinbach, J.R. Berendzen, and H. Frauenfelder (With 3 Figures) | 433 |
|--|-----|

Part VIII Energy Transfer and Relaxation

| | |
|---|-----|
| Energy and Electron Transfer of Adsorbed Dyes on Molecular Single Crystals and Other Substrates. By K. Kemnitz, N. Nakashima, and K. Yoshihara (With 5 Figures) | 438 |
| Optical Pump-Probe Spectroscopy of Dyes on Surfaces: Ground-State Recovery of Rhodamine 640 on ZnO and Fused Silica By P.A. Anfinrud, T.P. Causgrove, and W.S. Struve (With 1 Figure) | 442 |
| Picosecond Fluorescence Spectroscopy on Molecular Association in Langmuir-Blodgett Films By I. Yamazaki, N. Tamai, and T. Yamazaki (With 3 Figures) | 444 |
| Fluorescence Concentration Depolarization of DODCI in Glycerol: A Photon-Counting Test of Three-Dimensional Excitation Transport Theory By D.E. Hart, P.A. Anfinrud, and W.S. Struve (With 1 Figure) ... | 447 |
| Fractal Behaviors in Two-Dimensional Excitation Energy Transfer on Vesicle Surfaces. By N. Tamai, T. Yamazaki, I. Yamazaki, and N. Mataga (With 3 Figures) | 449 |
| Transient Vibrational Heating of Molecules After Internal Conversion. By A. Seilmeier, U. Sukowski, W. Kaiser, and S.F. Fischer (With 2 Figures) | 454 |
| Nonlinear Absorption Spectroscopy of Liquids with Ultrashort IR Pulses By H. Graener, R. Dohlus, and A. Laubereau (With 2 Figures) | 458 |
| Femtosecond Relaxation Dynamics of Large Organic Molecules By M.J. Rosker, F.W. Wise, C.L. Tang, and A.J. Taylor (With 4 Figures) | 461 |
| Population Lifetimes of OH($\nu=1$) and OD($\nu=1$) Vibrations in Alcohols, Silanols and Crystalline Micas. By E.J. Heilweil, M.P. Casassa, R.R. Cavanagh, and J.C. Stephenson | 465 |
| S_0 - S_n Two-Photon Absorption Dynamics of Rhodamine Dyes By P. Sperber, M. Weidner, and A. Penzkofer (With 3 Figures) | 469 |

| | |
|---|-----|
| Nonlinear Optical Response of One-Dimensional Excitons in Polydiacetylene. By B.I. Greene, J. Orenstein, R.R. Millard, and L.R. Williams (With 2 Figures) | 472 |
| Picosecond Photoconductivity and Nonlinear Optical Phenomena in <i>trans</i> -Polyacetylene By D. Moses, M. Sinclair, and A.J. Heeger (With 1 Figure) | 475 |
| Singlet Exciton Fusion in Molecular Solids By R.R. Millard and B.I. Greene (With 2 Figures) | 478 |
| Matrix Effect on Vibrational Relaxation in Molecular Crystals By J.R. Hill, E.L. Chronister, J.C. Postlewaite, and D.D. Dlott (With 1 Figure) | 482 |
| Optical Damage in Molecular Crystals: A Solid State Explosion By D.D. Dlott, T.J. Kosic, and J.R. Hill (With 4 Figures) | 485 |
| Rotational Relaxation of Free and Solvated Rotors By A.J. Bain, C. Han, P.L. Holt, P.J. McCarthy, A.B. Myers, M.A. Pereira, and R.M. Hochstrasser (With 5 Figures) | 489 |
| Ultrafast Dynamics at the Interface: Probing the Transition from Solution to Surface Interactions in Charged Micelles By E.F. Templeton, K. Brinker, S. Paone, and G.A. Kenney-Wallace (With 1 Figure) | 495 |
| Shock Moderated Photophysics and Photochemistry at Multi-kilobar Pressures By B.L. Justus, A.L. Huston, and A.J. Campillo (With 5 Figures) . | 499 |

Part IX Coherent Spectroscopic Techniques

| | |
|---|-----|
| Phase Grating Approach to Susceptibility Tensors: Determination in Isotropic Media. By J. Etchepare, G. Grillon, I. Thomazeau, G. Hamoniaux, and A. Orszag (With 4 Figures) | 504 |
| Nonlinear Response Function for Four-Wave Mixing: Application to Coherent Raman Lineshapes in Polyatomics and to the Optical Anderson Transition By S. Mukamel, Z. Deng, and R.F. Loring (With 2 Figures) | 510 |
| Picosecond Laser Pulse Shaping and Phase Shifting for Molecular Spectroscopy By M. Haner, F. Spano, and W.S. Warren (With 2 Figures) | 514 |
| Third-Order Nonlinear Optical Interactions in Thin Films of Organic Polymers Investigated by Picosecond and Subpicosecond Four-Wave Mixing. By P.N. Prasad, D. Narayana Rao, J. Swiatkiewicz, P. Chopra, and S.K. Ghoshal | 518 |

| | |
|---|------------|
| Picosecond Raman-Induced Phase Conjugation Spectroscopy By R. Dorsinville, P. Delfyett, and R.R. Alfano (With 2 Figures) .. | 521 |
| Polarization Dependence of Time-Resolved CARS in Liquids By N. Kohles and A. Laubereau (With 3 Figures) | 524 |
| Direct Measurement of Wave-Vector-Dependent Polariton Energy Velocity and Dephasing in NH_4Cl By G.M. Gale, F. Vallée, and C. Flytzanis (With 4 Figures) | 528 |
| Impulsive Stimulated Rayleigh, Brillouin, and Raman Scattering: Experiments and Theory of Light Scattering Spectroscopy in the Time Domain. By M.R. Farrar, L.R. Williams, Yong-Xin Yan, Lap-Tak Cheng, and K.A. Nelson (With 4 Figures) | 532 |
| Ultrafast Transient Spectroscopy with Broadband Non-Transform- Limited Light Sources By T. Yajima and N. Morita (With 4 Figures) | 536 |
| Picosecond Dephasing Time Measurement by CSRS Using Temporally Incoherent Nanosecond Laser with Short Correlation Time By T. Kobayashi, T. Hattori, and A. Terasaki (With 3 Figures) ... | 541 |
| Anomalous Pulse Duration Dependence of the Quasicontinuum Absorption Spectrum By P. Mukherjee and H.S. Kwok (With 3 Figures) | 544 |
| Index of Contributors | 549 |

Femtosecond Carrier Relaxation in Semiconductor-Doped Glasses

M.C. Nuss*, W. Zinth, and W. Kaiser

Physik Department der Technischen Universität München, Arcisstr. 21,
D-8000 München 2, Fed. Rep. of Germany

Semiconductor-doped glasses incorporating small $\text{CdS}_x\text{Se}_{1-x}$ or $\text{CdSe}_x\text{Te}_{1-x}$ crystallites in a glass matrix, show strong nonlinear absorption /1/ and large values of the nonlinear optical susceptibility χ_3 /2/. The semiconductor crystallite system currently attracts increasing attention when the semiconductor inclusions are small enough to expect quantum effects.

The semiconductor-doped glassfilters studied (Schott RG 830, RG 715, and RG 645) are characterized by an exponential absorption edge \sim three times less steep than the corresponding bulk semiconductors. The frequency position of the absorption edge varies with composition, but it may as well be influenced by the size of the semiconductor inclusions. No confinement effects are observed in the absorption spectra at 300 K, most probably due to a certain variation of crystallite size.

Femtosecond absorption recovery of all three Schott filter glasses was studied. In the experiment, femtosecond light pulses of \approx 60 fs duration and $\lambda = 620$ nm from a colliding-pulse modelocking dye laser generate an electron-hole plasma with a carrier density $N \approx 3 \times 10^{17} \text{ cm}^{-3}$ in the semiconductor inclusions. A weaker probing pulse samples the absorption changes as a function of the delay time between exciting and probing pulses. All data were recorded at room temperature.

Fig.1a,b shows the time-resolved absorption changes for the semiconductor-doped glass filters RG 645 and RG 830. The absorption change ΔA is plotted versus delay time between exciting and probing pulses. The dashed curves are the cross-correlation traces determining time zero. In the RG 830 semiconductor-doped glass (Fig.1b) the energy of the femtosecond laser pulses is well above the bandgap, creating carriers with an excess energy $\Delta E \approx 500$ meV. A fast recovery of the initial bleaching is observed with a time constant of 230 fs. This process can be identified with cooling of the initially hot electron gas to the lattice temperature. A comparison with the expected energy loss rate of the electron gas due to the emission of LO-phonons in crystalline semiconductors /3/ yields similar relaxation times for the absorption recovery. In RG 645 (Fig.1a) the opposite extreme is realized. The excess energy is only slightly larger than the bandgap. The absorption decreases with the integrated pulse intensity. No fast carrier relaxation process is observed since the carriers are injected with low excess energy. Consequently, the temperature of the electron gas will not change and no fast absorption recovery is observed. The bleaching is due to the filling of states in the conduction and valence bands and remains essentially constant over the plotted time.

*Present address: AT&T Bell Laboratories, 600 Mountain Ave.,
Murray Hill, N.J. 07974, USA

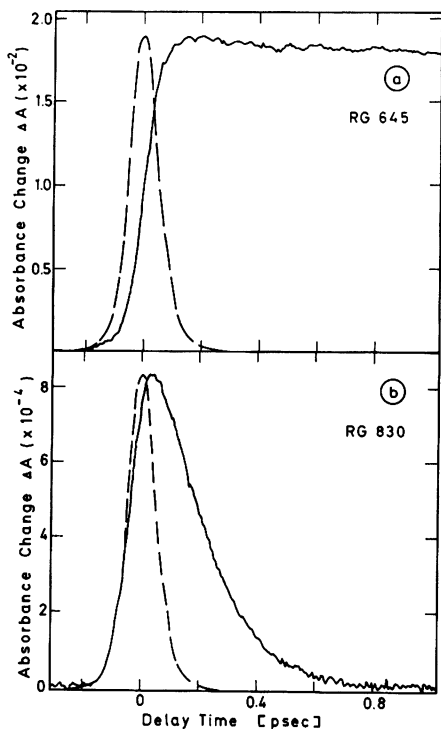


Fig.1 Femtosecond absorption recovery of semiconductor-doped glass filters RG 645 (Fig.1a) and RG 830 (Fig.1b).

Actually, ΔA decays with a long time constant of ~ 100 ps (not shown in the figure). We attribute the 100 ps time constant to electron-hole recombination. This short recombination time is not unreasonable in the light of the large number of surface states in the semiconductor-doped glasses, reacting as efficient recombination centers.

The most interesting case is the semiconductor-doped glass RG 715 (Fig.2), where the initial carrier excess energy ΔE is ~ 300 meV. Here, both the femtosecond decay process as well as the bandfilling can be traced. The three solid curves correspond to different excitation densities, where the lower curves are for two times (curve b) and four times (curve c) attenuated laser pulses, respectively. A semilog plot of the data reveals two time constants; 250 fs for the fast initial absorption recovery and 85 ps for the carrier recombination process. Significant is the superlinear decrease with carrier density of ΔA for times > 1 ps: ΔA decreases four times faster if the carrier density is reduced by a factor of 2.

The data can be explained assuming a carrier density dependent bandfilling process. In particular, we think of energy levels or traps below the conduction band, acting as a sink for the conduction band electrons. If the density of these levels is about the same as the carrier density ($\sim 10^{17}$ cm^{-3}) and the trapping time is several hundred femtoseconds, the capture of the carriers into these levels becomes saturated, leading to the nonlinear dependence of ΔA on carrier density observed in Fig.2. The fast 250 fs relaxation process is a combination of cooling of the electron gas due to LO-phonon emission and trapping of charge carriers. From there, electron-hole recombination takes place via surface states in the middle of the bandgap with a time constant of 85-100 ps.

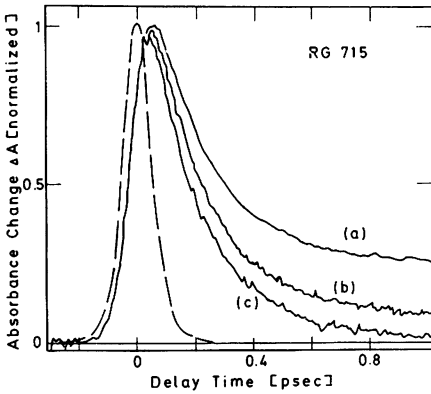


Fig.2 Absorption recovery of the semiconductor-doped glass RG 715

In conclusion, we point out that the absorption changes observed for the three semiconductor-doped glasses investigated here can be well explained within the framework of bulk semiconductor physics. The observed processes are cooling of a hot electron, electron trapping, and recombination. There is no indication of quantum size effects in the currently used glasses. We expect that excitonic effects will only be apparent for semiconductor-doped systems with smaller crystallites and with homogeneous size distribution.

- 1 G. Bret, F. Gires, Appl. Phys. Lett. 4 (1964) 175
B. Danielzik, K. Nattermann, D. von der Linde, Appl. Phys. B38 (1985), 31
- 2 R.K. Jain, R.C. Lind, J. Opt. Soc. Am. 73 (1983) 647
P. Roussignol, D. Ricard, K.C. Rustagi, C. Flytzanis, Optics Commun. 55 (1985) 143
- 3 J. Shah, Solid State Electron. 21 (1978) 43